crystals

MDPI

Article

Comparative Study on the Activity of GaF_3 and Ga_2O_3 Nanoparticle-Doped CsF-AlF_3 Flux for Brazing 6061 Al/Q235 Steel Joints

Zhen Yao, Songbai Xue * and Junxiong Zhang

College of Materials Science and Technology, Nanjing University of Aeronautics and Astronautics, Nanjing 210016, China; yaozhen123@nuaa.edu.cn (Z.Y.); zhangjunxiong126@163.com (J.Z.)

* Correspondence: xuesb@nuaa.edu.cn; Tel.: +86-025-8489-6070

Received: 6 May 2020; Accepted: 8 June 2020; Published: 9 June 2020

Abstract: The effect of trace amounts of GaF_3 and Ga_2O_3 nanoparticles on the wettability and spreadability of CsF-AlF_3 flux matched Zn-15Al filler metal were comparatively studied on 6061 aluminum alloy and Q235 low-carbon steel. The experimental results indicate that appropriate amounts of GaF_3 and Ga_2O_3 added into the flux could significantly promote the Zn-15Al filler metal to wet and spread on the surface of 6061 aluminum alloy and Q235 low-carbon steel. The optimum ranges for GaF_3 and Ga_2O_3 were 0.0075–0.01wt.% and 0.009–0.01 wt.%, respectively. Comparative analysis showed that the activity of CsF-AlF_3 flux bearing GaF_3 was higher than that bearing Ga_2O_3. The reason for this is that the former flux has a stronger ability to remove oxides of the base metal and reduce the interfacial tension of the molten filler metal and the base metal.

Keywords: spreadability; wettability; GaF_3; Ga_2O_3; CsF-AlF_3 flux

1. Introduction

Considering their excellent physical and chemical properties as well as good mechanical processability and corrosion resistance, aluminum alloys has become the most widely used non-ferrous metal structural materials in modern industries, including appliances, construction, light industry, storage tanks, aviation, aerospace, automobile and weapons. Among them, 6061 aluminum alloy has the advantages of excellent formability, welding performance, machinability and corrosion resistance [1,2]. Despite their outstanding properties, the mechanical strength of aluminum alloys is occasionally insufficient to meet the requirements of rigid structures such as car body keel, while the welding structure of aluminum and steel can effectively reduce the weight and additionally exhibit an enhanced strength. Therefore, the combination of aluminum alloy and steel shows great potential in the manufacturing industry.

Although the combination of aluminum alloy and steel plays an important role in the modern manufacturing industry, it remains a hot topic and difficult problem to obtain stable and reliable welded joints in the welding field, particularly for complicated situation in aluminum/steel dissimilar metals [3,4]. Domestic and foreign scholars were committed to the problem of aluminum steel welding in recent years and have proposed various welding approaches, such as cold metal transition brazing [5], aluminum alloy/galvanized steel MIG welding [6] and so on. The difficulties in the welding of aluminum/steel dissimilar metals is mainly related to the following two aspects: the different physical properties of aluminum and steel, which lead to considerable welding stress in the joints, and the brittle intermetallic compounds of the Fe-Al phase generated at the interface between aluminum and steel which exert a great impact on the mechanical properties of joints. The latter is the main contributor to a less reliable connection between aluminum and steel. Iron has a rather low solubility

in solid aluminum. When cooled at room temperature, Al-rich intermetallic compounds like Fe_4Al_{13}, $FeAl_3$, Fe_2Al_5 and $FeAl_2$ will be generated even with a small amount of iron. With the increasing content of iron, FeAl, Fe_3Al and other Fe-rich compounds will also be produced. These intermetallic compounds weaken the welded joint and reduce machinability. Therefore, it is of great importance to effectively suppress the generation of Fe-Al intermetallic compounds. Studies showed that adding trace Zr elements to the Zn-15Al welding matrix can reduce the thickness of the generated Fe_4Al_{13} intermetallic compounds and thus decrease the growth rate [7].

By joining method of brazing, the base metal is wetted with liquid filler metal and filling the joint gap. The working temperature is lower than the melting point of the base metal. Therefore, with brazing connection between aluminum and steel, the formation of intermetallic compounds can be effectively suppressed. In the case of brazing aluminum/steel heterogeneous metals, the use of flux is necessary except for vacuum brazing. At present, it is a general agreement that the main benefits of flux in the brazing process include removing oxide film and oil on the base metal surface and preventing further oxidation of the solder by covering the molten liquid solder so as to improve the spreadability and wettability of the brazing material. Currently, low eutectic Nocolock fluxes including KF-AlF_3 and CsF-AlF_3 [8] are widely used to braze aluminum alloys worldwide. This kind of flux has strong activity and can effectively remove the oxide film on the surface of aluminum alloy and promote the wetting and spreading of filler metal on the surface of aluminum and obtain the aluminum–aluminum brazing joint with excellent performance. However, it suffers from poor activity to iron oxide and difficulties in effective removal of the iron oxide film on the surface of carbon steel. Therefore, the liquid filler metal shows less favorable spreadability and wettability to the carbon steel base metal and it is difficult for the filler metal to produce a fine joint between the aluminum and carbon steel. It was confirmed that [9] by adding a small amount of RbF, the activity of CsF-AlF_3 flux on the surface of stainless steel, the oxide film can be improved significantly. With the addition of 0.5 wt.% RbF into CsF-AlF_3 flux, the brazing joint of 6063 aluminum alloy and 304 stainless steel exhibits a tensile strength of up to 127 MPa. Adding 0.5 wt.% Zr [10,11] into Zn-15Al filler metal has an obvious fining effect on the η-Zn phase of the matrix. When the mass fraction of Zr is up to 0.2%, the optimal effect is achieved while the shear strength of brazing joint is up to 143 MPa.

A previous investigation [12] proved that the addition of Ga_2O_3 nanoparticles could significantly improve the performance of CsF-RbF-AlF_3 flux while brazing aluminum alloy to carbon steels. The strengthening mechanism can be mainly attributed to the production of Ga element and its enrichment at the base metal/filler metal interface during brazing. In this paper, the influence of doping trace GaF_3 and Ga_2O_3 nanoparticles into CsF-AlF_3 flux on the spreadability and wettability of Zn-15Al filler metal on the base metals was studied, and enhancement effects of these two nanoparticles on the flux activity were discussed and compared.

2. Materials and Methods

The base metals used in this work were the 6061 aluminum alloy and the Q235 steel, and the compositions of these two materials are respectively listed in Tables 1 and 2. The filler metal was Zn–15Al alloy. A series of CsF–AlF_3–GaF_3 fluxes with different contents of GaF_3 were prepared by using 99.9% GaF_3 flux and GaF_3 of AR purity, and the variation range of GaF_3 is 0.0001–0.1 wt.%. Nano Ga_2O_3 powder in the range of 0.0001–0.1 wt.% were added into the commercial CsF-AlF_3 flux to obtain a series of CsF–AlF_3–Ga_2O_3 fluxes. As an advance preparation, all the filler metal alloys were extruded as a wire with a 2 mm diameter. The base metals for the spreading test were processed into plates with the dimensions of 40 mm × 40 mm × 3 mm in advance. All the specimens and filler metals were mechanically polished using SiC paper. In addition, the above-mentioned experimental materials were degreased with acetone and cleaned using ethanol before brazing.

Table 1. Chemical composition of 6061 aluminum alloy (wt.%).

Alloy	Mg	Si	Cu	Cr	Mn	Zn	Al
6061	1.10	0.61	0.25	0.12	0.01	0.01	Bal.

Table 2. Chemical composition of Q235 steel (wt.%).

Alloy	C	Mn	Si	S	P	Fe
Q235	0.18	0.48	0.30	0.04	0.04	Bal.

The spreading test was carried out strictly in accordance with China's National Standard GB 11364-2008. In this process, 0.1 g filler metal was accurately weighted and placed on the Q235 steel or 6061 aluminum alloy covered with the prepared CsF–AlF_3–GaF_3 flux or CsF–AlF_3–Ga_2O_3 flux and then carefully put into an electrical resistance furnace as Figure 1. The heating temperature was set at 530 °C and the holding time was 1 min. After the test, the flux residues were collected from the surface of the base metal with clean tweezers and the components in the residues were analyzed with an XRD diffractometer (Brucker D8). CuKα radiation was used in the test, with the voltage of 40 kV, the current of 110 mA, and the scanning speed of 1 °/min. The brazing alloy sample should be polished before test. A 3 mm × 3 mm sample was cut on one side of the brazed joint and used for XRD analysis after cleaning. Then, ultrasonic wave waits were incorporated to clean the test board of base material and calculate the spreading area. In order to ensure the accuracy of the test results, the above tests were repeated 5 times under the same conditions, and the results were averaged.

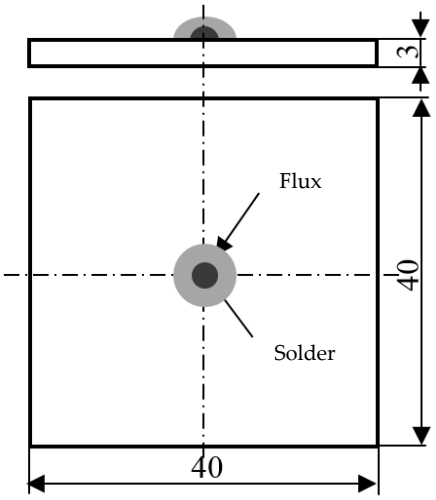

Figure 1. Schematic diagram of the spreading test.

3. Results and Discussion

3.1. The Spreadability and Wettability of Zn-15Al Filler Metal

The effect of GaF_3 and Ga_2O_3 particles on the spreadability of Zn-15Al filler metal was evaluated by the spreading tests that were carried out on the surface of 6061 aluminum alloy and Q235 low-carbon steel with aid of the prepared flux bearing nanoparticles. The spreading areas were measured and averaged. Figure 2a showed the relationship between the concentration of GaF_3 and Ga_2O_3 and spreading area on 6061 aluminum alloy. When the concentration of GaF_3 was 0.01 wt.%, the maximum spreading area of Zn-15Al on 6061 aluminum alloy was 328 mm^2, which is 64% higher than that without GaF_3 addition (200 mm^2). The maximum spreading area of Zn-15Al on 6061 aluminum alloy was 319 mm^2 and was increased by 60% compared with that without doping Ga_2O_3 into the flux, while the concentration of Ga_2O_3 was 0.009 wt.%.

Figure 2b indicates that the spreadability of Zn-15Al filler metal over Q235 steel than Ga_2O_3 was clearly improved by the addition of GaF_3 into the CsF-AlF_3 flux. When the concentration of GaF_3 was 0.0075 wt.%, the maximum spreading area of Zn-15Al on 6061 aluminum alloy was 188 mm^2. When the concentration of Ga_2O_3 was 0.01 wt.%, the maximum spreading area of Zn-15Al on 6061 aluminum alloy was 160 mm^2. Under this circumstance, by adding GaF_3, the spreading area of Zn-15Al filler metal over Q235 steel was increased by 104% comparing to that of CsF-AlF_3 flux (92 mm^2) and by 17.5% comparing to the addition of Ga_2O_3.

Considering the spreading of Zn-15Al filler metal on both 6061 aluminum alloy and Q235 low-carbon steel, the optimum ranges for GaF_3 and Ga_2O_3 in CsF–AlF_3 flux were 0.0075–0.01 wt.% and 0.009–0.01 wt.%, respectively.

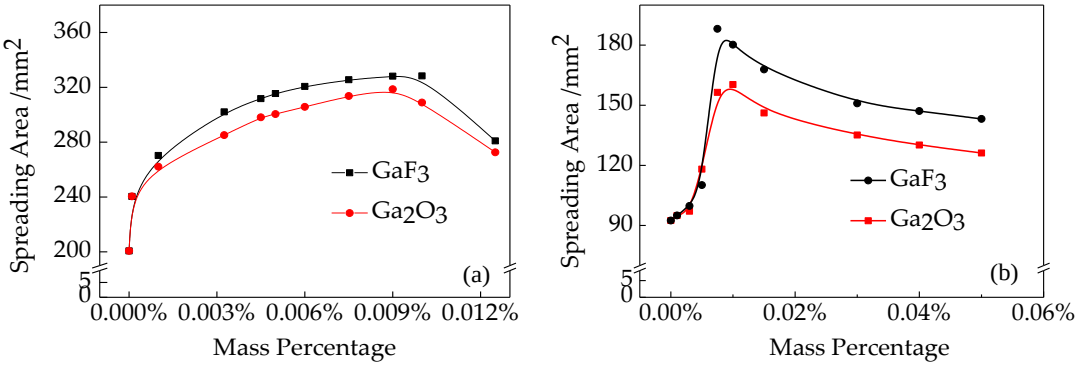

Figure 2. Spreading area of Zn-15Al filler metal (**a**) 6061 aluminum alloy; (**b**) Q235 low-carbon steel.

3.2. The Mechanism of Interfacial Reaction

The CsF-AlF_3-GaF_3 flux could effectively improve the spreadability of Zn-15Al filler metal over 6061 aluminum alloy and Q235 steel, but how it worked was not clear yet and deserved a detailed investigation. Therefore, the theory of interfacial tension was applied reasonably to confirm some potential explanations. On the basis of the Young's equation illustrated by Figure 3 and Equation (1), the liquid balance over solid surface was determined by the interfacial tensions between solids, liquids and gases. Specifically, these interfacial tensions could be summed up as between base metal and molten flux (γ_{SF}), molten filler metal and molten flux (γ_{LF}) and base metal and molten filler metal (γ_{SL}) in this study.

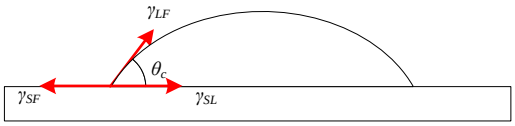

Figure 3. Diagrammatic sketch of Young's equation.

Non-reactive wetting and reactive wetting were two approaches to wetting a solid with molten metal, and the interfacial tension between the base metal and molten filler metal (γ_{SL}) decreased due to the reaction and the spreading was improved. Because the molted flux reacted with the surface metallic oxides over the base metal and removed them, the reactive wetting was what we discussed in this research. While balancing, the relationship of interfacial tensions is shown as Equation (1).

$$\gamma_{SF} = \gamma_{LF} \times \cos\theta + \gamma_{SL} \quad (1)$$

$$\gamma_{SF} > \gamma_{LF} \times \cos\theta + \gamma\prime_{SL} \quad (2)$$

Alumina reacted with melted XF-AlF_3 (X = Na, K, Rb, Cs) flux and formed AlF_3 to be dissolved, and the interfacial tension of solid–liquid (γ_{SL}) changed from Zn-Al alloy-alumina to

Zn-Al alloy-aluminum [13]. The remarkable intersolubility of Zn and Al made the interfacial tension between AA6061 and Zn-15Al alloy (γ_{SL}) decrease rapidly and the spreading area of Zn-15Al alloy over AA6061 increased significantly under this condition. However, no research has reported that the CsF-AlF_3-based flux could react with iron oxide immediately and the surface oxide was still the largest obstacle. The phase diagram of Fe-Zn showed that intermetallics, such as FeZn and $FeZn_4$, formed below 600 °C. It could be included that the Zn-15Al filler metal spread over Q235 steel made γ'_{SL} decreased gradually by the reaction of Zn and Fe.

The wetting angles of different fluxes over AA6061 are shown in Table 3. Molten Zn-Al filler metal wetted AA6061 alloy and Q235 steel and spread on the base metal, which reduced the γ_{SL} shown in Equation (2) and the balance of Young's equation was broken. The new flux breaks the tension balance of the original interface and thus the spreading area of Zn-15Al is promoted with the addition of GaF_3. Ga^{3+} ion in GaF_3 has a "skin effect", which is analogous to the chemical representation of a thin layer of electrical current concentrated on the outer surface of a conductor, and its small surface tension can significantly reduce γ_{SL}. Due to the enrichment of Ga^{3+} ions, γ_{SL} decreases rapidly, while the spreading area of the liquid filler metal increases further. However, with the consumption of liquid flux, the ability to remove the Al_2O_3 oxide film gradually weakens and finally the reactivity disappears. The interfacial tension (γ_{SF}) between the base metal and flux decreases. The equilibrium of interfacial tension in Equation (1) is reassumed. The spreading area of filler metal attains saturation and the spreading shape is fixed.

Table 3. Wetting angles of different fluxes.

Flux	$CsF\text{-}AlF_3$	$CsF\text{-}AlF_3\text{-}Ga_2O_3$	$CsF\text{-}AlF_3\text{-}GaF_3$
Wetting angle θ	27.44	19.43	17.71
cosθ	0.89	0.94	0.95
Spreading area/mm^2	200	319	328
Wetting coefficient W	178.0	299.9	311.6

It could be demonstrated that Ga^{3+} was released from GaF_3, whose reaction equation was Equation (3), considering the activity of molten Zn-15Al filler metal. Ga could permeate into the molten filler metal spontaneously with its similar chemical property to Al. The EDX (Energy Dispersive X-ray Spectroscopy) results are shown in Figure 4, and it can be seen that in the interface of base metal and filler metal, a weak peak of Ga appeared. Original balance was broken and the spreading area increased significantly because of the decrease in γ_{SL}. The diagrammatic sketch of the interfacial tension of spread Zn-Al filler metal is shown as Figure 5.

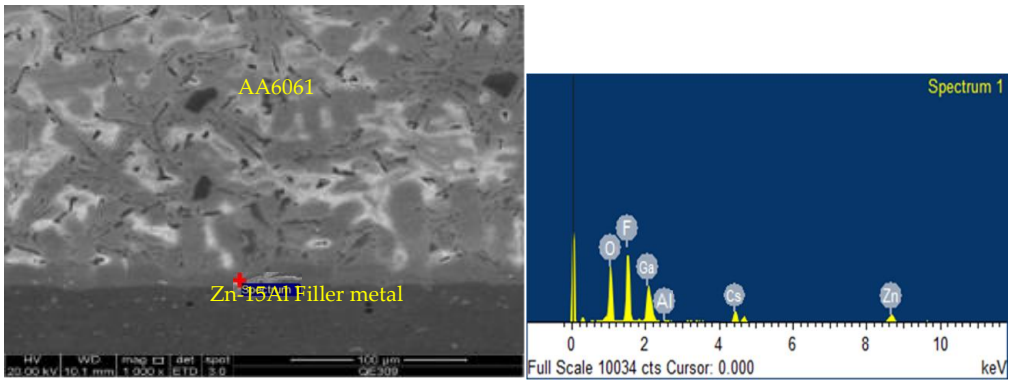

(**a**) (**b**)

Figure 4. EDX results of the interface of AA6061 and Zn-15Al filler metal: (**a**) SEM scanning image; (**b**) EDX results of the section.

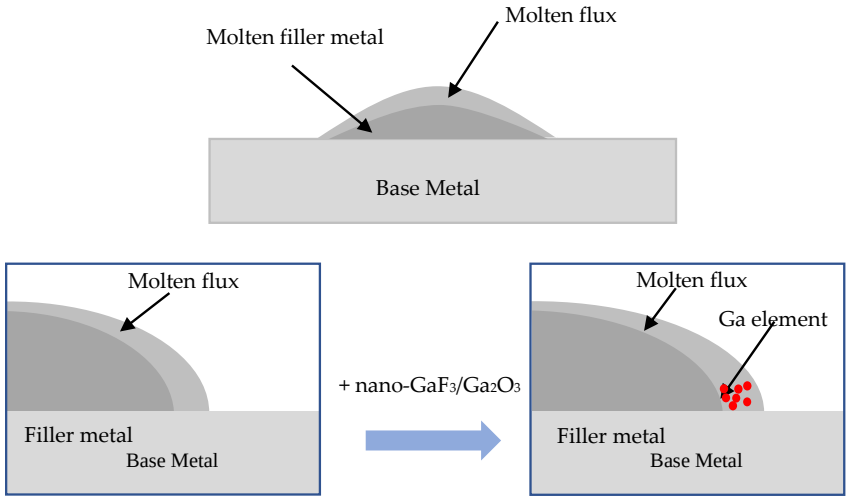

Figure 5. Diagrammatic sketch of the interfacial tension of spread Zn-Al filler metal.

The XRD results of the flux residue were shown in Figure 6. It revealed the residue products over AA6061 were $MgMnSi_2O_6$, Al_2SiO_5, $MgSiO_3$, Zn_2SiO_4, CuO, Cu_4O_3, Al_2O_3, $Cs_{11}O_3$, AlF_3, MnF_2 and $ZnGa_2O_4$, and which were Al_2SiO_5, Fe_2SiO_4, $AlPO_4$, $FePO_4$, Al_2O_3, ZnO, SiO_2, AlF_3, MnF_2 and $MnAlF_5$ over Q235 steel.

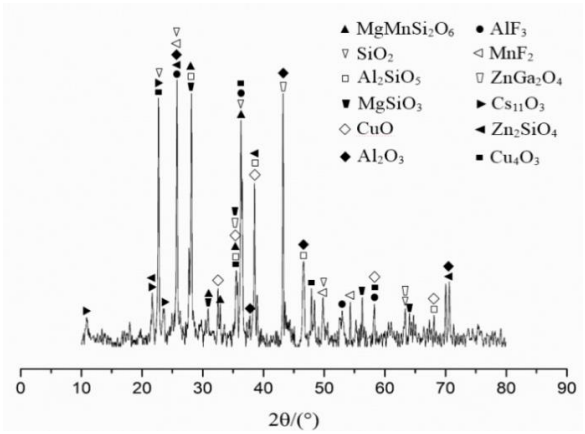

(**a**)

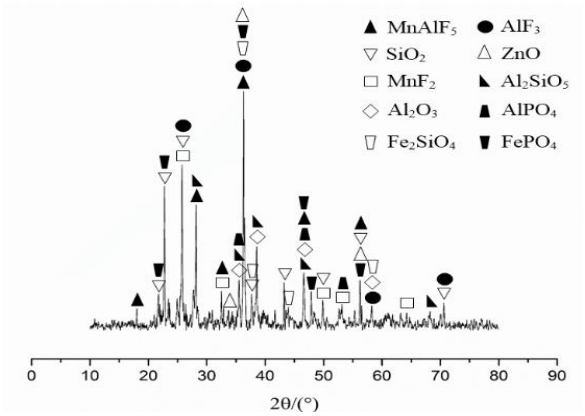

(**b**)

Figure 6. XRD analysis results of flux residua: (**a**) 6061 aluminum alloy; (**b**) Q235 low-carbon steel.

The compounds over AA6061 surface were mainly made up of Mg_2Si, MgO, $MgAl_2O_4$, amorphous Al_2O_3 and a little Cu, Mn, Cr, Fe according to report [14]. The content of Mg, Mn and Si increased while over 520 °C. Figure 6 reveals that the $Cs_{11}O_3$, silicate and fluoride came from the reaction between the oxide and flux. It could be confirmed that $ZnGa_2O_4$ arose from the residue of the trace amounts of GaF_3 in the flux. It was reported [15] the additional Ga tended to enrich on the surface, which led to the speculation that GaF_3 might be involved in some kind of reaction. Because of this, $ZnGa_2O_4$ was validated to show its diffraction peaks in the XRD pattern, whose reaction equation is Equation (4).

$$GaF_3 \rightarrow Ga^{3+} + 3F^- \tag{3}$$

$$4ZnO + 2GaF_3 \rightarrow ZnGa_2O_4 + 3ZnF_2 \tag{4}$$

$$ZnO + Ga_2O_3 \rightarrow ZnGa_2O_4 \tag{5}$$

$$CsFAlF_4 \overset{\Delta}{\leftrightarrow} CsF + AlF_3 \tag{6}$$

$$F^- + Al_2O_3 \rightarrow AlF_3 + O^{2-} \tag{7}$$

$$F^- + Fe_2O_3 \rightarrow FeF_3 + O^{2-} \tag{8}$$

The mechanism for alumina removal from CsF-AlF_3 flux was the dissolution and reaction of the active ingredients such as F^-, HF, SiF_6^{2-} and Zn^{2+} ions. Zn^{2+} and SiF_6^{2-} ions were liable to be generated during the spreading test because of the massive amount of Zn in the filler metal and a little Si on the base metal surface. The major flux reaction is listed in Equation (5), which refers to the flux with the addition of Ga_2O_3 nanoparticles. In addition, trace amounts of H_2O, NH_4F and NH_4AlF_4 appeared in the CsF-AlF_3-GaF_3 flux, which produced HF and further promoted the removal.

According to Figure 6, the XRD result of residue over Q235 steel was not the same as that in AA6061. Research showed that Fe_2O_3, Fe_3O_4 and FeO were distributed systematically on Q235 steel [16]. Thus, the removal of iron oxide was the primary step. According to the XRD result shown in Figure 6, the reaction of SiO_2, iron oxide and alumina formed Fe_2SiO_5 and Al_2SiO_5. MnF_2 and $MnAlF_5$ were formed by the reaction between F^-, HF, Mn compounds and AlF_3. However, the appearance of a trifle phosphate, $FePO_4$ and $AlPO_4$ in the XRD result led to the conclusion that $FePO_4$ and $AlPO_4$ were formed as Equation (9), under the condition that no phosphorus was contained in the flux and its content was below 0.04 wt.% in Q235 steel.

$$Me_2O_3 + P_2O_5 \rightarrow 2MePO_4 (Me = Fe,\ Al) \tag{9}$$

$$Fe_2O_3 + 2Al \rightarrow Al_2O_3 + 2Fe \tag{10}$$

Because the content of phosphorus in Q235 could not be detected by the XRD, it meant that P enriched over Q235 surface, which was a normal phenomenon occurring when heating P-containing alloys such that the phosphorus was burnt out, producing phosphorus oxide. Although the existence of P removed a little of the metallic oxide, it was insufficient to remove all oxide films. Therefore, it was clear that the main reaction mechanism of removing metallic oxides referred to the reaction between Al and iron oxide as Equation (10).

Because of the large concentration of Al and Zn elements in the Zn-Al filler metal, the surface oxide film of the filler metal and Q235 steel is prone to react and the oxide film can be effectively removed. Fe, Cr, Ni and other elements obtained by the reaction were then rapidly dissolved into Q235 steel base material, so Al_2O_3 and ZnO were detected in large quantities in the reaction residue, which reasonably explained the XRD results in Figure 6.

$$36CsF + 2SiO_2 + 6HF + 5MnO \rightarrow 2Cs_{11}O_3 + 2Cs_2SiF_6 + 5Cs_2MnF_6 + 3H_2O \uparrow \tag{11}$$

The reaction shown in Equation (11) explains the decrease in the flux activity due to the huge consumption of the CsF and its lowered flowability. The formation of Ga^{3+} enhanced the spreadability of Zn-15Al filler metal while leading to less activity.

According to the proposed mechanisms, molten flux reacted with oxide and the spread of filler metal was promoted simultaneously. Nevertheless, the efficiency of alumina removal was decreased by the rapid effective loss of molten flux and the spreading speed of Zn-15Al was further delayed. The reason could be the consumption of active substances such as SiF_6^{2-}, HF and F^-, and the production of silicates.

Different from the lower efficiency of CsF-AlF_3 flux on iron deoxidation, the addition of GaF_3 significantly improved the activity on account of the enrichment and production of Ga^{3+}, and thus decreased the interfacial tension between base metal and Zn-15Al [17]. In addition, the dissolving reaction between GaF_3 with ZnO occurred and consequently the spreading of molten Zn-15Al was further promoted.

Instead of reacting and producing Ga^{3+} for the addition of GaF_3, Ga_2O_3 tends to react with ZnO to produce $ZnGa_2O_4$ according to Equation (5). Meanwhile, when nano-Ga_2O_3 particles were added into the flux as a chemical agent, Ga element can only be released by the reaction of Zn-Al alloy and Ga_2O_3 particles. As a typical spinel oxide, $ZnGa_2O_4$ belongs to a cubic crystal system and the chemical stability and thermal stability are very high [18]. Accordingly, more energy is needed to separate Ga from Ga_2O_3. The formation of $ZnGa_2O_4$ somehow facilitates the release of active substances, such as F and Al, which remove the oxide film on the surface of the 6061 Al alloy and the Q235 steel.

Combining the above issues with the XRD results shown in Figure 6, it was speculated that the main reactions are shown as Equations (3)–(11). The formation of active substances such as SiF_6^{2-}, HF and F^- helped the molten flux remove the surface oxide over AA6061, and the iron oxide over Q235 steel was removed by active Al in the filler metal and enriched element P, which led to the improvement in the spreadability of molten Zn-15Al on the base metal.

3.3. Comparative Analysis on the Effect of GaF_3 and Ga_2O_3 Addition

Combined with the analysis of the enhancement mechanism of doping Ga_2O_3 nanoparticles into the flux in a previous study [12], it can be concluded that surface-active Ga obtained from the reaction of the flux and base metals during brazing plays a major enhancement role in promoting the spreading of Zn-Al filler metal on the base metal.

As an ionic compound, GaF_3 consists of cations Ga^{3+} and anions F^-, which means Ga^{3+} and F^- ions can be dissociated more easily from GaF_3 than Ga_2O_3 when heated. The dissociation product Ga^{3+} can rapidly and effectively reduce the interfacial tension between the Zn-15Al filler metal and the base metal to further promote the spreadability of the filler metal. In addition, the synergistic effect of GaF_3 can promote the surface enrichment of P element according to the above "skin effect" and partially remove the surface oxide film of Q235 carbon steel, which further improve the spreadability of the filler metal. Meanwhile when nano-Ga_2O_3 particles were added into the flux as a chemical agent, Ga can only be released by the reaction of Zn-Al alloy and Ga_2O_3 particles. Therefore, compared with GaF_3, more energy is needed to separate Ga from Ga_2O_3 during brazing.

Compared with the results of previous analysis [12,19], the addition of GaF_3 and Ga_2O_3 in this study increases the spreading area of the filler metal on both 6061 aluminum alloy and Q235 steel, and the flux bearing GaF_3 has better activity than that bearing Ga_2O_3.

4. Conclusions

In this study, trace amounts of GaF_3 and Ga_2O_3 nanoparticles were respectively added into CsF-AlF_3 flux for brazing aluminum to carbon steels. The effects of these two nanoparticles on the flux activity and the spreadability of Zn-15Al filler metal on the base metal were comparatively investigated. The major conclusions were as follows:

(1) The spreading tests showed that with the addition of trace amounts of GaF_3 and Ga_2O_3 in CsF-AlF_3 flux, the spreadability of Zn-15Al filler metal both on Q235 steel and AA6061 alloy was effectively improved, and the enhancement effect of GaF_3 was more obvious. The optimal contents of GaF_3 and Ga_2O_3 were 0.0075–0.01 wt.% and 0.009–0.01 wt.%, respectively.

(2) The "skin effect" of GaF_3 improved the activity of fluxes by reacting with Al atoms to produce Ga^{3+}, and enrichment of Ga^{3+} on molten filler metal decreased the interfacial tension and enlarged the spreading area of molten Zn-15Al filler metal on the base metals.

(3) In addition, as an ionic compound, GaF_3 could easily react and generate Ga^{3+} to promote the enrichment of P element in the base metal to remove the oxide film on Q235 carbon steel and promote the wetting of the filler metal. Therefore, the activity of CsF-AlF_3 flux with the addition of GaF_3 was higher than that with the addition of Ga_2O_3.

Author Contributions: Conceptualization, S.X.; methodology, J.Z.; software, Z.Y.; validation, Z.Y.; formal analysis, Z.Y.; investigation, Z.Y.; resources, S.X.; data curation, Z.Y.; writing—original draft preparation, Z.Y.; writing—review and editing, Z.Y.; visualization, Z.Y.; supervision, S.X.; project administration, S.X.; funding acquisition, S.X. All authors have read and agreed to the published version of the manuscript.

Funding: This research was funded by the National Natural Science Foundation of China, Grant No. 51375233 and the Priority Academic Program Development of Jiangsu Higher Education Institutions (PAPD).

Acknowledgments: We gratefully acknowledge the support of Jiangsu Higher Education Institutions for providing a scholarship for Zhen Yao. Songbai Xue acknowledges financial support from the National Natural Science Foundation of China, Grant No. 51375233.

Conflicts of Interest: The authors declare no conflict of interest.

References

1. Choi, C.Y.; Kim, D.C.; Nam, D.G. A Hybrid Joining Technology for Aluminum/Zinc Coated Steels in Vehicles. *Mater. Sci. Technol.* **2010**, *26*, 858–964. [CrossRef]
2. Gale, W.F.; Butts, D.A. Transient liquid phase bonding. *Sci. Technol. Weld. Join.* **2004**, *9*, 283–300. [CrossRef]
3. Yu, S.; Ling, S.; Jiankang, H.; Yufen, G. Performance of $Fe_2A_5Zn_{0.4}$ in Interface of Aluminum and Galvanized Steel Welding-Brazing and Its Formation. *Rare Met. Mater. Eng.* **2013**, *42*, 432–436.
4. Jing, Y.; Xiaoyan, L.; Li, C.; Shuili, G.; Qiaoyan, L. Microstructure and Properties of Twin Spot Laser Welded Joints of 1420 Al-Li Alloy. *Rare Met. Mater. Eng.* **2011**, *40*, 871–874.
5. Jinglong, Y.; Songbai, X.; Peng, X.; Wei, D.; Zhaoping, L.; Man, Z. Microstructure and mechanical properties of aluminum stainless steel brazed joint with torch brazing. *Trans. China Weld. Inst.* **2015**, *36*, 63–66.
6. Zhen, L.; Xuyou, W.; Aiqing, Y.; Guoliang, Q.; Wei, W.; Shangyang, L. Research on Fusion-Brazing Joining between Aluminum and Steel by Laser-MIG Hybrid Welding. *Rare Met. Mater. Eng.* **2009**, *38*, 229–233.
7. Jinglong, Y.; Songbai, X.; Ducan, P.S. An Impact of Zirconium Doping of Zn-Al Braze on the Aluminum-Stainless Steel Joints Integrity During Aging. *J. Mater. Eng. Perform.* **2017**, *26*, 358–365.
8. Songbai, X.; Ling, Z.; Zongjie, H.; Xiang, H. Reaction mechanism between oxide film on surface of Al-Li alloy and CsF-AlF_3 flux. *Trans. Nonferrous Met. Soc. China* **2008**, *18*, 121–125.
9. Jinglong, Y.; Songbai, X.; Peng, X.; Zhaoping, L.; Wei, D.; Junxiong, Z. Development of novel CsF–RbF–AlF_3 flux for brazing aluminum to stainless steel with Zn–Al filler metal. *Mater. Des.* **2014**, *64*, 110–115.
10. Jinglong, Y.; Songbai, X.; Peng, X.; Zhaoping, L.; Weiming, L.; Guangxing, Z.; Qingke, Z.; Peng, H. Development of Zn–15Al–xZr filler metals for Brazing 6061 aluminum alloy to stainless steel. *Mater. Sci. Eng. A* **2016**, *651*, 425–434.
11. Jinglong, Y.; Songbai, X.; Peng, X.; Zhaoping, L. Effect of zirconium on microstructure and properties of Zn-15Al filler metal. *Trans. China Weld. Inst.* **2016**, *12*, 61–65.
12. Zhen, Y.; Songbai, X.; Jinlong, Y.; Junxiong, Z. Inducing the Effect of a Ga_2O_3 Nano-Particle on the CsF-RbF-AlF_3 Flux for Brazing Aluminum to Carbon Steels. *Crystals* **2020**, *10*, 183.
13. Haidong, Q.; Haiyan, G.; Jun, W.; Baode, S. Recent Researches and Development of Brazing Flux for Aluminum. *Mater. Rev.* **2007**, *12*, 76–79.
14. Junxiong, Z.; Songbai, X.; Peng, X.; Shuang, L. Thermodynamic reaction mechanism of the intermetallic compounds of SnxNdy and GaxNdy in soldered joint of Sn–9Zn–1Ga–0.5Nd. *J. Mater. Sci.* **2015**, *26*, 3064–3068.

15. Hong, Z.; Songbai, X.; Zhong, S. Mechanism of CsF-AlF_3 and KF-AlF_3 fluxes reacting with oxide films of 6063 aluminum alloy. *Trans. China Weld. Inst.* **2009**, *30*, 13–16.
16. Yi, W.; Dun, Z.; Huaiqun, L.; Yongjuan, L.; Baorong, H. Influence of sulphate-reducing bacteria on environmental parameters and marine corrosion behavior of Q235 steel in aerobic conditions. *Electrochim. Acta* **2010**, *55*, 1528–1534.
17. Qiyun, Z.; Sunqi, L.; Dongqi, L.; Liangchun, Y. Effect of trace additive on anti-oxidation of molten SN-Pb eutectics. *Trans. China Weld. Inst.* **1984**, *20*, 296–302.
18. Yanbo, J.; Shujie, J.; Shiyong, C.; Dongbo, W.; Jinzhong, W. Synthesis and Photocatalytic Activity of $ZnGa_2O_4$ Nanocubes. *China J. Lumin.* **2019**, *40*, 49–56.
19. Junxiong, Z.; Songbai, X.; Peng, X.; Jinlong, Y.; Zhaoping, L. Effect of Ga_2O_3 on the Wettability and Spreadability of CsF-RbF-AlF_3 Flux/Zn-Al Filler Metal on Aluminum and Steel. *Rare Met. Mater. Eng.* **2017**, *46*, 1900–1904.